# Using modern coexistence theory to understand community disassembly

Joe Brennan[1,2,*]

Sebastian J. Schreiber[1,2]

1. Department of Evolution and Ecology, University of California, Davis USA 95616;

2. Center for Population Biology, University of California, Davis USA 95616;

∗ Corresponding author; e-mail: jlbrennan@ucdavis.edu.

Co-author email: sschreiber@ucdavis.edu

Short running title: Community disassembly and coexistence theory

*Keywords*: community disassembly, secondary extinction, coexistence theory, competition, facilitation, keystone predation

Article Type: Letter

Statement of Authorship: J. Brennan and S.J. Schreiber conceived the idea. JB performed the computational analyses, created the figures, and drafted the manuscript with feedback from SJS. SJS performed the mathematical analyses with feedback from JB. JB and SJS reviewed and edited manuscript drafts.

Data accessibility statement: Code needed to recreate analyses can be found on J. Brennan's GitHub account at `https://github.com/biologyjoe87/ident_quant_sec_ext`. No new data was generated in this study.

Abstract word count: 150

Number of words in main text: 4566

Number of figures: 6

Total number of citations: 82

**Abstract**

Community disassembly examines how species extinction alters ecological communities. Sometimes, the extinction of one species can trigger the loss of others, known as secondary extinction. These secondary extinctions often result from complex species interactions, complicating the identification of underlying mechanisms. Here, we leverage Modern Coexistence Theory to identify when and why secondary extinctions occur. To identify when secondary extinctions occur, we introduce the Community Disassembly Graph, that uses invasion growth rates to identify transitions between coexisting communities due to extinction. When a secondary extinction is identified, we decompose the invasion growth rates associated with the secondary extinction to understand why it occurs. We demonstrate the utility of this framework by applying it to models in which different species interactions – competition, facilitation, and predation – contribute significantly to secondary extinctions. Our results show Modern Coexistence Theory offers a flexible and interpretable approach to understanding when and why secondary extinctions occur.

# Introduction

Species participate in a complex, entangled web of interactions, such that the extinction of one species can significantly alter the structure and dynamics of an ecological community. These cascading impacts due to species extinction, known as community disassembly, has become a central focus for understanding biodiversity change (Ostfeld and LoGiudice, 2003; Zavaleta et al., 2009). In some cases, the extinction of a single species can trigger cascading effects that ultimately drive other species extinct (Paine, 1966; Lubchenco, 1978; Ebenman and Jonsson, 2005; Jordán, 2009; Langendorf et al., 2025), known as secondary extinction (Brodie et al., 2014). Secondary extinctions are speculated to contribute significantly to the loss of diversity globally under anthropogenic change in a wide variety of taxa (Moir et al., 2010; Colwell et al., 2012; Strona and Bradshaw, 2018; Kehoe et al., 2021).

When there is a strong direct dependency of one species on another species, the cause of secondary extinction is often clear. This is the case for predators that rely on their prey or obligate mutualists that depend on their partners. Most theoretical studies of community disassembly focus on these direct dependencies. A common approach to identify secondary extinctions uses static food webs or mutualist networks where interactions between species are modeled, but changes in species densities are ignored. To study disassembly in these models, practitioners remove a node corresponding to a species and all associated edges corresponding to some species interaction (predation and obligate mutualism, respectively) and declare that species with no more resources or mutualists experience secondary extinction (Dunne et al., 2002b; Memmott et al., 2004; Bane et al., 2018). These studies have provided important insights into how the structure of ecological networks impact the community disassembly process (Dunne et al., 2002b, 2004; Bascompte and Stouffer, 2009; Tang et al., 2024).

Although these studies provide a level of tractability that is difficult to achieve in dynamic models, they neglect well-established mechanisms of secondary extinction that arise from indirect effects. For example, Paine (1966) studied changes in diversity of a rocky intertidal community following removal of the top predator *Pisaster ochraceus*. This loss of predation led to unregulated growth of the prey species *Mytilus californianus* and *Mitella polymerus*, ultimately leading to the secondary extinction of six other species. These secondary extinctions would not

be predicted by the static approach as *P. ochraceus* was neither a mutualist nor resource. Only by studying the strength of the interactions and associated dynamics of the community can one understand what led to the dramatic reduction in diversity after the loss of the keystone predator *P. ochraceus* (Paine, 1980; Paine et al., 2010). Secondary extinctions have been also attributed to the loss of other indirect mechanisms such as ecosystem engineering (Wright et al., 2002; Yeakel et al., 2020) and intransitive competition (Jackson and Buss, 1975; Kerr et al., 2002; Edwards and Schreiber, 2010). The exclusion of these indirect mechanisms of secondary extinction biases our understanding of community disassembly and can lead to underestimates of secondary extinctions. By incorporating both direct and indirect mechanisms into community disassembly studies, we can more accurately predict the susceptibility of ecological communities to secondary extinctions.

However, identifying the main drivers of secondary extinctions can be complicated by the cumulative impact of multiple ecological drivers and interactions between these factors (Colwell et al., 2012; Brodie et al., 2014). A secondary extinction might occur from the impact of multiple competitors or from a single dominant competitor. For example, in systems with a single limiting resource, one species alone can be sufficient to exclude others (Gause, 1934; Tilman, 1982). In contrast, microbial communities with trade-offs in growth traits can allow all pairs of species to coexist but not the full community (Manhart and Shakhnovich, 2018), implying that multiple competitors are needed for exclusion of a single species. In such cases of emergent exclusion, disentangling the relative importance of ecological mechanisms is required to understand why the secondary extinction occurred.

Modern Coexistence Theory (MCT) is an increasingly popular framework that quantifies how multiple, interacting ecological mechanisms influence coexistence outcomes. MCT's key metric is the invasion growth rate (IGR), defined as the per capita growth rate of an invading species at low density while other species are at some coexistence state. MCT decomposes this IGR to identify what mechanisms promote the successful invasion of the species (Chesson, 1994; Barabás et al., 2018; Ellner et al., 2019). However, these same techniques can also explain what mechanisms most strongly impede successful coexistence or result in invasion failure (Grainger et al., 2019a; Shoemaker et al., 2020; Spaak and Schreiber, 2023). Therefore,

we can leverage MCT to quantify the mechanisms that enable persistence of the secondarily extinct species in the full community with the keystone species, but lead to their exclusion in the post-extinction community.

Here, we identify when and why secondary extinctions occur using techniques from MCT. To identify when secondary extinctions occur, we use the concept of "$-i$ communities" from MCT to define the Community Disassembly Graph that describes how extinctions alter community composition. To understand why the secondary extinction occurs, we decompose and compare invasion growth rates using the methods of MCT to identify the ecological drivers responsible for the secondary extinction.

# Methods

## The Community Disassembly Graph

To model the dynamics of ecological communities, we use deterministic differential and difference equations where $x_i(t)$ denotes the density of species $i$ at time $t$. The differential equations take the form $\frac{dx_i}{dt} = x_i f_i(x)$ where $f_i(x)$ is the per-capita growth rate of species $i$ at community state $x = (x_1, x_2, \ldots, x_n)$. The discrete-time models take the form $x_i(t+1) = x_i(t)F_i(x(t))$ where $F_i(x)$ is the per-capita fitness at community state $x$. For the discrete-time models, $f_i(x) = \ln F_i(x)$ corresponds to the per-capita growth rate of species $i$. For these models, there are various ways to define coexistence (Schreiber, 2006; Clark et al., 2024). Here, we define coexistence as a feasible attractor (Clark et al., 2024). Namely, there exists a steady state (or more generally an invariant set) at which all the species densities are positive and the species return to this steady state following sufficiently small perturbations of the species densities. Similarly, for any subset of species, coexistence occurs if the model restricted to those species has a feasible attractor.

When a set of species in a community coexist, the extinction of a species, say species $i$, typically results in the community dynamics settling to a new feasible attractor for the system without species $i$. These attractors are known as a $-i$ communities (Chesson, 1994; Hofbauer and Schreiber, 2022). For a given set of coexisting species, we can identify the $-i$ community

for each species in the community. If all coexisting communities and their $-i$ communities are known, then one can summarize their relationships in a Community Dissassembly Graph. In this graph, directed edges are drawn from each set of coexisting species (the vertices) to each of their $-i$ communities. Paths along this graph correspond to the changes in community composition due to species removals. A directed edge corresponds to a secondary extinction if the $-i$ community loses more than species $i$.

## Using IGRs to identify $-i$ communities and secondary extinctions

We can solve for $-i$ communities using IGRs, defined as the per-capita growth rate of a species when rare and resident species are at stationarity (Hofbauer and Schreiber, 2022). For differential equations, the IGR of species $i$ at some coexistence state equals

$$\lim_{T\to\infty} \frac{1}{T} \int_{t=0}^{T} f_i(x(t))dt$$

while for difference equations, they equal

$$\lim_{T\to\infty} \frac{1}{T} \sum_{t=0}^{T} \ln F_i(x(t))$$

IGRs are typically used to identify if a species can successfully invade a coexisting community. If the IGR of a species is positive, the invading species can successfully invade the community, typically leading to some change in community composition (see, however, Mylius et al. (1998) and Mylius and Diekmann (2001) for the resident strikes back phenomenon). If the IGR of a species is negative, upon introduction into the community, the species abundance will decay to extinction.

Let $S \subseteq \{1, 2, \ldots, n\}$ be a subset of coexisting species. Hofbauer and Schreiber (2022) showed that a community $T$ is a $-i$ community of community $S$ if $T \subseteq S\backslash\{i\}$ and all species present in community $S$ but not in community $T$ disregarding species $i$ – that is, $T\backslash(S\backslash\{i\})$ – have a negative IGR at community $T$ . Secondary extinctions occur when species in $S$, other than possibly species $i$, have a negative IGR at community $T$.

## Decomposing invasion growth rates to determine the causes of secondary extinction

Having identified a secondary extinction event from the Community Disassembly Graph, we want to understand the relative importance of ecological factors underlying this event. To identify their relative importance, we apply the MCT approach to the two IGRs associated with the secondary extinction event. Say species $j$ went extinct following the loss of species $i$. We know that species $j$ then has a negative IGR at the $-i$ community. To understand why species $j$ has a negative IGR at the $-i$ community, we can decompose its IGR to quantify what aspects of the system impede its establishment. There exist several ways to decompose IGRs (Chesson, 1994; Ellner et al., 2019). Here, we use the method proposed by Ellner et al. (2019) because of its flexibility and broad applicability. The method assesses how different ecological factors impact the IGR of the invading species relative to the resident species. If one of these factors is comparatively more beneficial (or less harmful) to the invading species than to the resident competitors, this factor positively contributes to the IGR of the invading species. If the attribute is comparatively more beneficial (or less harmful) to the resident competitors than the invading species, it contributes negatively to the IGR of the invading species (Ellner et al., 2019). Identifying the relative contributions of ecological factors resulting in species $j$'s IGR being negative identifies the relative importance of these ecological factors in preventing species $j$ from establishing in the $-i$ community.

Although this identifies why species $j$ cannot persist following the loss of species $i$, it does not explain how species $i$ promotes persistence of species $j$. Thus, we also identify the $-j$ community and decompose the IGR of species $j$ at the $-j$ community. If the pre-extinction community coexists under the permanence criterion, then species $j$ will have a positive IGR at the $-j$ community (Hofbauer and Schreiber, 2022; Schreiber, 2025). By decomposing the IGR of species $j$ at the $-j$ community, we can understand what attributes of the system in the $-j$ community that are not in the $-i$ community allow species $j$ to invade successfully.

We employ this framework in three different models, each in which different species interactions help maintain coexistence of the full system: competition, facilitation, and predation. In each of these cases, the species interaction contributes significantly to the persistence of

the full community, and thus, following loss of the species mediating this interaction, another species experiences extinction. These three examples demonstrate the flexibility and utility of our approach.

# Applications

## Competition

Historically, competition has been viewed as a species interaction that prevents species from coexisting within a community (Armstrong and McGehee, 1980; Pastore et al., 2021). However, competition can also promote coexistence by suppressing the densities of competitively dominant species, allowing otherwise inferior competitors to persist (Edwards and Schreiber, 2010; Levine et al., 2017). To illustrate this type of indirect facilitation, we analyze an empirically parameterized model of a competitive annual plant community (Van Dyke et al., 2022).

Van Dyke et al. (2022) examined how coexistence outcomes change under different precipitation regimes. The model tracks annual seed production. The seeds germinate with some probability $g_i$ or go into the seed bank. If seeds enter the seed bank, they survive with probability $s_i$ to the next year. For the seeds that germinate, they then compete with other germinated individuals and then produce seeds. Under these assumptions, Van Dyke et al. (2022)'s model is

$$x_{i,t+1} = (1 - g_i)s_i x_{i,t} + \frac{g_i \lambda_i x_{i,t}}{1 + \sum_j a_{ij} g_j x_{j,t}} := x_{i,t} F_i\left(x\right)$$

For illustrative purposes, we focus on the model parametrized to the ambient rain scenario for a subset of species: *Acmispon wrangelianus*, *Hordeum murinum*, and *Plantago erecta* (parameters in Appendix A). To create the Community Disassembly Graph for this model, we find all coexistence states analytically (see Appendix A). Each single species coexistence state corresponds to a globally stable equilibrium. Only one pair of species (*A. wrangelianus* and *H. murinum*) can coexist and when they do, they coexist at a globally stable equilibrium (Appendix A). Finally, we use the invasion graph approach (Appendix A) to prove all three species

can coexist in the sense of permanence (Hofbauer and Schreiber, 2022).

Next, we evaluate each species' IGR at each coexistence state. Since each coexistence state corresponds to a globally-stable equilibrium $x^* = (x_1^*, x_2^*, x_3^*)$, the IGR of species $i$ at this equilibrium equals

$$\ln F_i\left(x^*\right) = \ln\left((1-g_i)s_i + \frac{g_i\lambda_i}{1+\sum_j a_{ij}g_jx_j^*}\right)$$

Using these IGRs, we identify all $-i$ communities and compute the Community Disassembly Graph (Figure 1A).

This Community Disassembly Graph identifies two secondary extinction events: the secondary extinction of *A. wrangelianus* following the loss of *H. murinum* and the secondary extinction of *P. erecta* following the loss of *A. wrangelianus* (Figure 1A). We focus here on understanding why *P. erecta* goes extinct following the extinction of *A. wrangelianus*. Appendix D analyzes the other case. To determine the cause of the secondary extinction event, we examine (1) what factors prevent *P. erecta* from establishing when only *H. murinum* is present and (2) what factors allow *P. erecta* to invade when *A. wrangelianus* is present in the community with *H. murinum*. Specifically, the factors of interest are competition against *P. erecta*, indirect impacts of competition between *A. wrangelianus* and *H. murinum* on *P. erecta* , and interactive effects between these direct and indirect effects.

*P. erecta* has a negative IGR at the *H. murinum* community (i.e., the -*A. wrangelianus* community), as it undergoes a secondary extinction following removal of *A. wrangelianus*. Our decomposition of this IGR (Figure 2) shows, as expected, the direct impact of competition from *H. murinum* on *P. erecta* is why this IGR is negative.

To understand why *P. erecta* can invade with *H. murinum* only in the presence of *A. wrangelianus*, we decompose its IGR at the *A. wrangelianus*–*H. murinum* community i.e. the $-$ *P. erecata* community. Individually, the direct impacts of competition from *H. murinum* and *A. wrangelianus* have large negative impacts on the IGR of *P. erecta* (second and third peach bars from the top in Figure 2). These negative impacts, however, are substantially reduced by the non-additive effects of competition on *P. erecta* and the indirect effects of these resident species competing. Importantly, this relatively small increase of direct competition is overcompensated

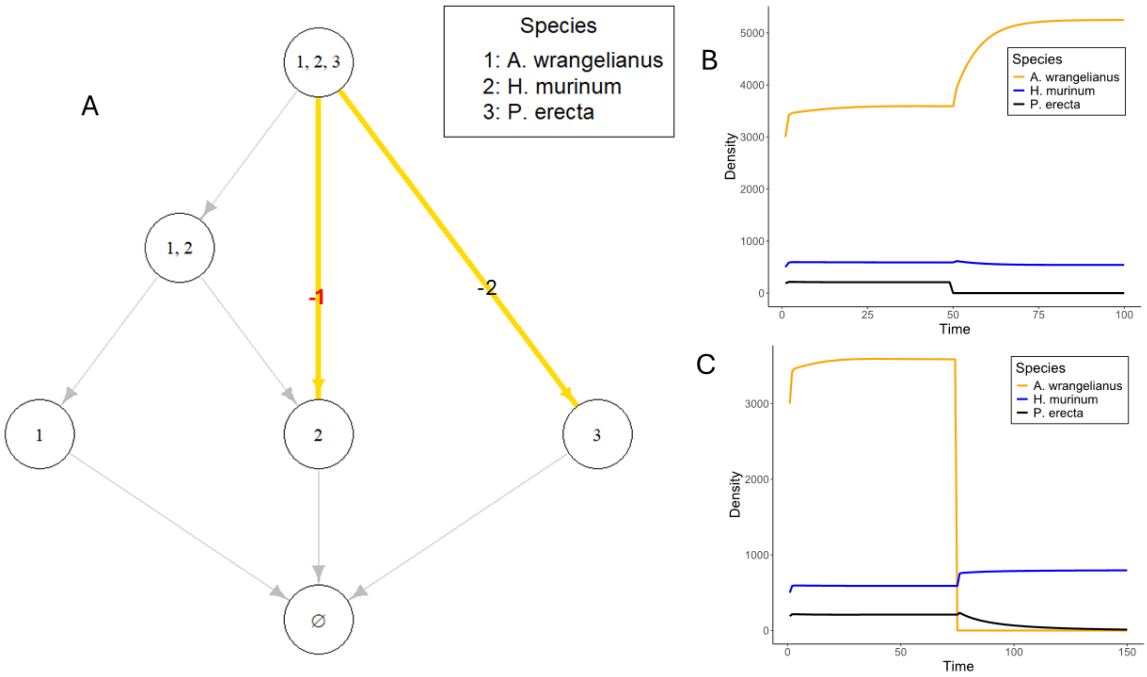


Figure 1: (A) Community Disassembly Graph of the annual plant community. Vertices depict coexisting subcommunities. Directed edges represent transitions from one community to another due to extinction of the labeled species. Extinctions resulting in no secondary extinctions are denoted by grey directed edges with no edge label while those containing secondary extinctions are in yellow with a corresponding edge label. The secondary extinction of interest is denoted by a red edge label. (B) Simulation of community dynamics following extinction of *P. erecta* at time step 50. Note that there are no secondary extinction events, matching the -*P. erecta* predicted in the Community Disassembly Graph. (C) Simulation of community dynamics following extinction of *A. wrangelianus* at time step 75. *P. erecta* decays towards extinction following the extinction of *A. wrangelianus*, confirming the secondary extinction predicted on the Community Disassembly Graph.

by competition between *A. wrangelanius* and *H. murinum* having a positive effect on *P. erecta* (positive peach bars). The competition between *P. erecta*'s two competitors and subadditivity of competition against *P. erecta* ultimately drives the IGR to be positive, allowing for successful invasion and, in this case, coexistence.

This analysis identifies the cause of *P. erecta*'s secondary extinction. In the community with *H. murinum* and *A. wrangelianus*, competition between *H. murinum* and *A. wrangelianus* suppresses their competitive dominance over *P. erecta*, permitting *P. erecta* to coexist within the full community. Consequently, the extinction of *A. wrangelianus* removes this competitive suppression of *H. murinum*, allowing *H. murinum* to competitively exclude *P. erecta*.

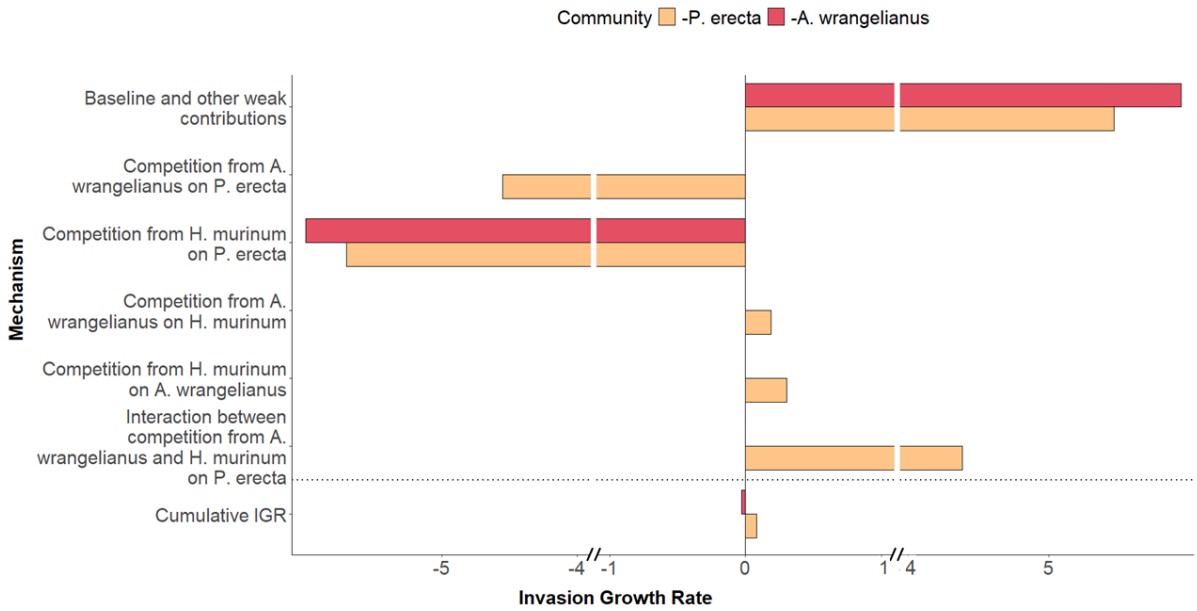


Figure 2: Decomposition of *P. erecta*'s IGR at the $-$*P. erecta* and $-$*A. wrangelianus* communities. The sum of all bars of a respective color above the dotted line add to the value of the bar below the dotted line of the respective color. Mechanisms whose value is less than $0.01$ were lumped into the baseline bar. Mechanisms not present in the $-i$ community have no contribution to the IGR and thus have no bar represented.

## Facilitation

Facilitation can buffer species' densities against negative interactions such as predation (Glynn, 1976; Stachowicz and Hay, 1999) and competition (Pennings and Callaway, 1996; Stachowicz, 2001). However, reliance on facilitative or mutualist interactions for persistence can increase vulnerability to secondary extinctions (Aslan et al., 2013; Vanbergen et al., 2017).

For instance, Geijzendorffer et al. (2011) empirically parametrized a series of Lotka-Volterra models to a grassland system exhibiting both competitive and facilitative interactions. In these models, each species $i$ has an intrinsic rate of growth, $r_i$, and a per-capita impact $a_{ji}$ on species $j$. If $a_{ji}$ is negative, species $i$ has a competitive effect on species $j$ while if positive, species $i$ facilitates species $j$. The model is

$$\frac{dx_i}{dt} = x_i \left( r_i + \sum_j a_{ij} x_j \right) := x_i f_i(x)$$

We focus on the parameterization for spring in Appendix B and consider a subset of species:

*Agrostis stolonifera*, *Lolium perenne*, *Phleum pratense*, *Trifolium pratense*, and *Trifolium repens*.

Using the invasion graph method (Hofbauer and Schreiber, 2022), we identify all coexistence states of the model (Appendix B). All of these coexistence states are not only local attractors, but global attractors i.e. permanent communities. Next, we evaluate the IGR of each species at each coexistence state. Due to the time averaging property of Lotka-Volterra models (Hofbauer and Sigmund, 1998), we can analytically solve for each IGR by evaluating at the respective equilibrium $x^* = (x_1^*, \ldots, x_5^*)$ i.e.,

$$f_i(x^*) = r_i + \sum_j a_{ij} x_j^*$$

Using this information, we computed the Community Disassembly graph (Figure 3A). This analysis reveals that all five species coexist and the existence of eight possible secondary extinctions events. Half of the secondary extinction events occur following the extinction of *T. repens* which causes the secondary extinction of *T. pratense*. This suggests that *T. repens* plays a crucial role in allowing *T. pratense* to coexist with other species in multiple contexts.

To understand these secondary extinctions, we focus on the secondary extinction of *T. pratense* when *T. repens* is removed from the entire community. To understand why this secondary extinction event occurs, we must address two key questions: (1) what factors prevent *T. pratense* from successfully invading the community with *A. stolonifera*, *L. perenne*, and *P. pratense* (i.e., in the -*T. repens* community), and (2) what factors allow *T. pratense* to successfully invade the community with these species if *T. repens* is present (i.e., in the -*T. pratense* community)? Specifically, we quantify the contributions of species interactions on the IGR of *T. pratense* relative to its impact on *T. pratense*'s competitors. We group the species interactions into four categories: the direct effects of competition and facilitation on *T. pratense* and the indirect effects of competition and facilitation on competitors of *T. pratense*.

To understand why *T. pratense* can not establish in the $-$*T. pratense* community, we decompose its negative IGR when the other species are equilibrium. We find that direct effects of competition and the indirect effects of facilitation among the competitors outweigh the indirect effects of competition among competitors. This results in a negative IGR for *T. pratense*. How-

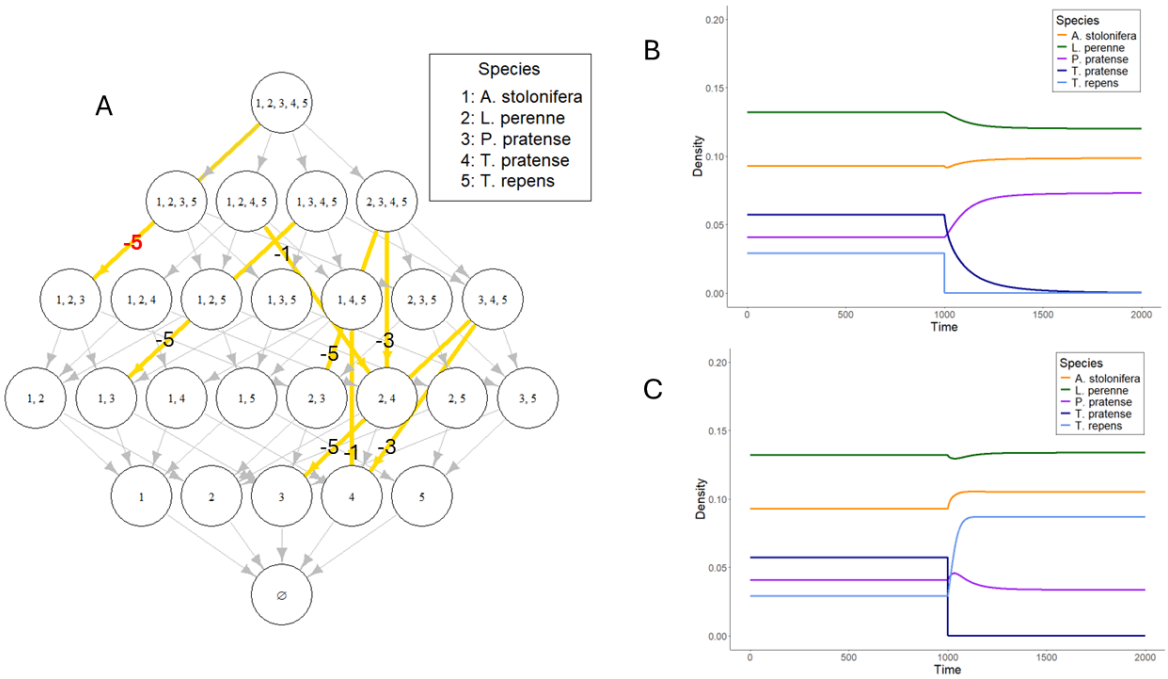


Figure 3: (A) Community Disassembly Graph of the grassland community. Vertices depict co-existing subcommunities. Directed edges represent transitions from one community to another due to extinction of the labeled species. Extinctions resulting in no secondary extinctions are denoted by grey directed edges with no edge label while those containing secondary extinctions are in yellow with a corresponding edge label. The secondary extinction of interest is denoted by a red edge label. (B) Simulation of community dynamics following extinction of *T. repens* at time step 1000. *T. pratense* decays towards extinction following the extinction of *T. repens*, confirming the secondary extinction predicted on the Community Disassembly Graph. (C) Simulation of community dynamics following extinction of *T. pratense* at time step 1000. Note that there are no secondary extinction events, matching the -*T. pratense* predicted in the Community Disassembly Graph.

ever, without the indirect effect of facilitation among competitors, the IGR would be positive. Hence, facilitation among the competitors plays a crucial role in the competitive exclusion of *T. pratense*.

Next, we examine how the presence of *T. repens* permits the establishment of *T. pratense*. Unlike in the $-$*T. repens* community, direct facilitation on *T. pratense* confers a significant positive contribution to its IGR. Additionally, competition against *T. pratense* is less harsh in the $-$*T. pratense* community than in the $-$*T. repens* community. In the $-$ *T. pratense* community, indirect effects due to competition and facilitation are stronger. However, since they have opposing effects on the IGRs of the same magnitude, the net impact of these indirect effects are negligible on *T. pratense*'s IGR. These mechanisms allow for *T. pratense* to have a positive IGR in the $-$*T. pratense* community unlike in the $-$*T. repens* community.

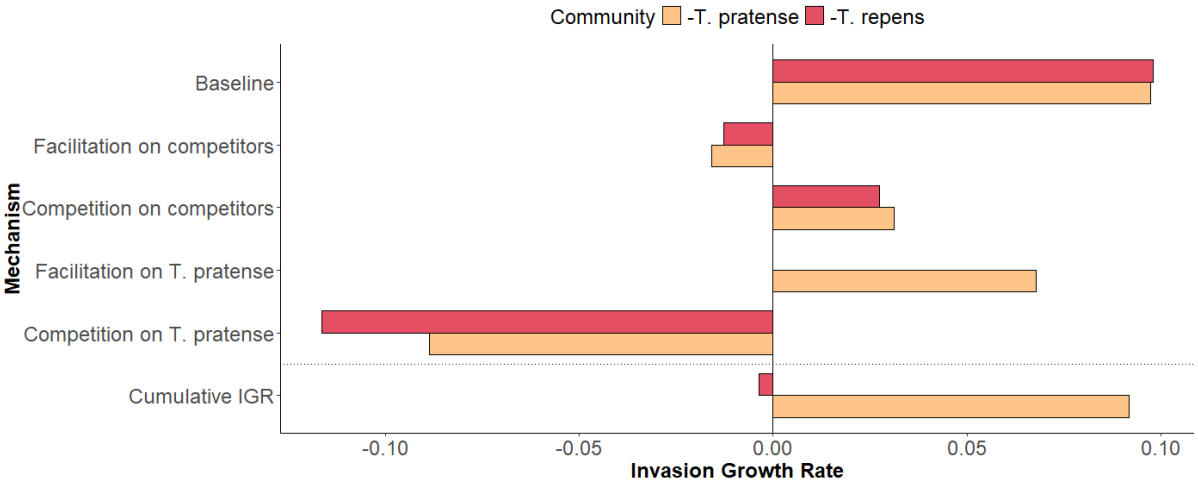


Figure 4: Decomposition of *T. pratense*'s IGR at the $-$*T. pratense* and $-$*T. repens* communities. The sum of all bars of a respective color above the dotted line add to the value of the bar below the dotted line of the respective color. Mechanisms not present in the $-i$ community have no contribution to the IGR and thus have no bar represented.

These decompositions imply that the secondary extinction of *T. pratense* following loss of *T. repens* was primarily driven by the loss of facilitation and stronger competitive pressure against *T. pratense*. In the full community, *T. repens*'s facilitation permits *T. pratense* to persist despite competitive pressures. However, following the extinction of *T. repens*, *T. pratense* becomes unable to withstand the competition from the remaining species in the disassembled community due to the strengthened direct competition against *T. pratense* and the indirect effect of facilitation among its competitors.

## Predation

Predation can maintain coexistence by regulating competitively dominant prey species– an effect known as keystone predation (Paine, 1966; Letnic et al., 2009; Wallach et al., 2015). A well-studied model of keystone predation is the diamond model with a basal resource ($R$), two competitors ($C_1$ and $C_2$) competing for the basal resource, and a top predator ($P$) that predates on both competitors (McCann et al., 1998; Schreiber and Rittenhouse, 2004; Vasseur and Fox, 2007; Shoemaker et al., 2020). Following Vasseur and Fox (2007)'s model formulation and

parameterization in Appendix C, the dynamics are

$$
\begin{aligned}
\frac{dP}{dt} &= -M_P P + J_P P \frac{\Omega_{PC_1} C_1 + (1-\Omega_{PC_1}) C_2}{\Omega_{PC_1} C_1 + (1-\Omega_{PC_1}) C_2 + C_0} \\
&:= P \cdot f_P(R, C_1, C_2, P) \\
\frac{dC_1}{dt} &= -M_{C_1} C_1 + \Omega_{C_1 R} J_{C_1} C_1 \frac{R}{R + R_{0_1}} - J_P P \frac{\Omega_{PC_1} C_1}{\Omega_{PC_1} C_1 + (1-\Omega_{PC_1}) C_2 + C_0} \\
&:= C_1 \cdot f_{C_1}(R, C_1, C_2, P) \\
\frac{dC_2}{dt} &= -M_{C_2} C_2 + \Omega_{C_2 R} J_{C_2} C_2 \frac{R}{R + R_{0_2}} - J_P P \frac{(1-\Omega_{PC_1}) C_2}{\Omega_{PC_1} C_1 + (1-\Omega_{PC_1}) C_2 + C_0} \\
&:= C_2 \cdot f_{C_2}(R, C_1, C_2, P) \\
\frac{dR}{dt} &= rR\left(1 - \frac{R}{K}\right) - \Omega_{C_1 R} J_{C_1} C_1 \frac{R}{R + R_{0_1}} - \Omega_{C_2 R} J_{C_2} C_2 \frac{R}{R + R_{0_2}} \\
&:= R \cdot f_R(R, C_1, C_2, P)
\end{aligned}
$$

Due to the complexity of the model, we use numerical simulations to identify all coexistence states involving two or more species. For each subset of two or more species, we run a set of simulations with each of those species at initially positive densities. We run the dynamics until they reach stationarity and identify which species successfully coexist. We define coexistence as all species at initially positive density having an average density greater than $10^{-9}$ after the burn-in period to the end of the time series. For each set of species, we test multiple sets of initial conditions to identify other attractors if they exist. For this parameterization, we only identified at most one attractor for each coexisting subsystem.

To calculate the IGR for a given coexistence state, we numerically integrated the model using the deSolve package in the programming language R (Soetaert et al., 2010) evaluated at time intervals of $\Delta t = 0.1$ with a burn-in time of $1,000$ and a total run time of $10,000$. We approximate the IGR for species $i$

$$
\lim_{T \to \infty} \frac{1}{T} \int_{t=0}^{T} f_i(R(t), C_1(t), C_2(t), P(t)) dt
$$

by the Riemann sum

$$\sum_{k=10,000}^{100,000} f_i(R(k\Delta t), C_1(k\Delta t), C_2(k\Delta t), P(k\Delta t))\Delta t$$

for $i \in \{R, C_1, C_2, P\}$.

Using the numerically identified coexistence states and the associated IGRs, we calculate the model's invasion graph (Appendix C) and Community Disassembly Graph (Figure 5). Under the parametrization studied in Vasseur and Fox (2007) and Shoemaker et al. (2020), we find several secondary extinctions (Figure 5A). Most of the secondary extinctions are intuitive (loss of resource leads to loss of species directly dependent on the resource). However, two are more interesting: extinction of the predator $P$ induces secondary extinction of the second consumer $C_2$ and the extinction of the first consumer $C_1$ induces the secondary extinction of the predator $P$. Here, we study how the extinction of $P$ induces the secondary extinction of $C_2$. We consider three ecological factors: relative nonlinearity in response to resource fluctuations, predator preference ($\Omega_{PC_1}$), and the resident consumer's utilization of the shared resource ($J_{C_1}$).

First, we assess why consumer 2 $C_2$ has a negative IGR in the community with only the resource $R$ and the other consumer $C_1$. As expected, the utilization of the resource by $C_1$ is the primary factor that makes $C_2$'s IGR negative (fourth red bar in Figure 6). We find that fluctuations in $R$ have a negative impact on the IGR of $C_2$, but that the interaction between fluctuations in $R$ and $C_1$'s intake of $R$ has a positive impact on $C_2$'s IGR due to its negative impact on $C_1$. This positive contribution, however, does not offset the negative contributions of each factor independently, resulting in a negative IGR of $C_2$.

Next, we examine why $C_2$ can establish in the presence of the predator $P$. To do this, we decompose the IGR of $C_2$ at the $-C_2$ community. Decomposing the IGR of $C_2$, we find that, yet again, fluctuations in $R$ and $C_1$'s use of $R$ have negative contributions to the IGR while their interaction has a weak, positive contribution (peach bars in 6). The effect of predator preference is sufficiently positive to counteract the negative contributions of fluctuations in $R$ and $C_1$'s utilization of $R$. This confirms our hypothesis that successful invasion of $C_2$ is

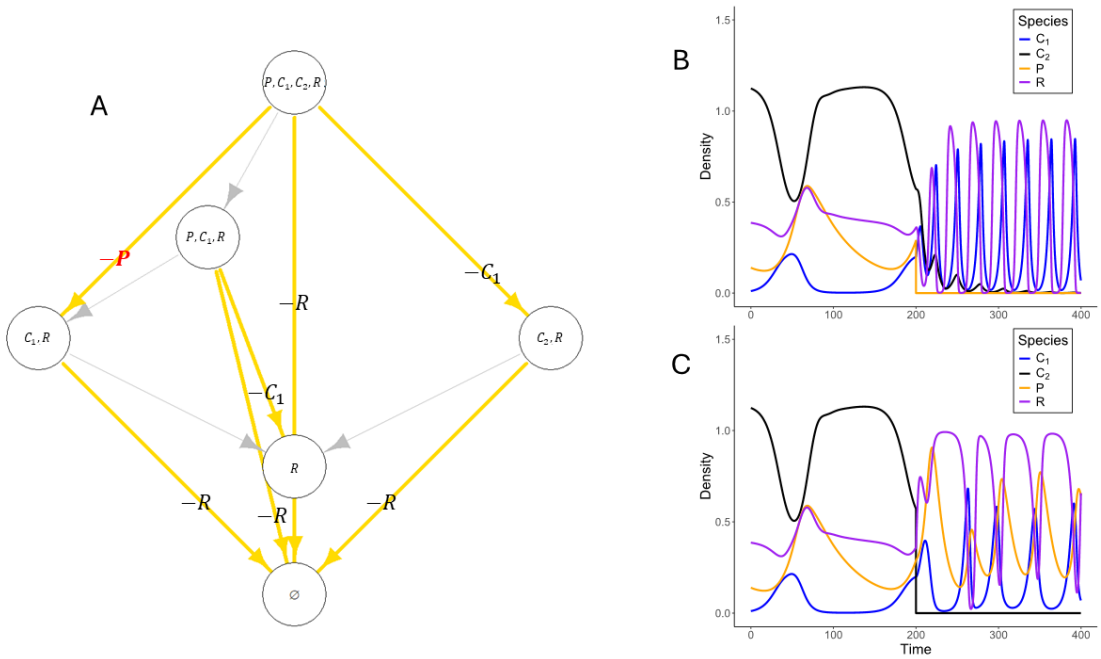


Figure 5: (A) Community Disassembly Graph of the diamond model. Vertices depict coexisting subcommunities. Directed edges represent transitions from one community to another due to extinction of the labeled species. Extinctions resulting in no secondary extinctions are denoted by grey directed edges with no edge label while those containing secondary extinctions are in yellow with a corresponding edge label. The secondary extinction of interest is denoted by a red edge label. (B) Simulation of community dynamics following extinction of $P$ at time step 200. $C_2$ decays towards extinction following the extinction of $P$, confirming the secondary extinction predicted on the Community Disassembly Graph. (C) Simulation of community dynamics following extinction of $C_2$ at time step 200. Note that there are no secondary extinction events, matching the -$C_2$ predicted in the Community Disassembly Graph.

dependent on $P$'s presence and, crucially, its preference for consuming $C_1$.

Comparing the two IGR decompositions, we find that the predator's presence made baseline conditions and resource fluctuations more beneficial for $C_2$ while making the impact of $C_1$'s resource utilization and the interaction between these factors more detrimental for $C_2$. In addition to changing these pre-existing factors, the predator's preference serves as a positive factor resulting in a positive IGR.

Synthesizing these results, when $P$ is present, its preferential consumption of $C_1$ sufficiently suppresses $C_1$'s competitive dominance over $C_2$, enabling coexistence of all species. However, the extinction of $P$ eliminates the top down control on $C_2$. Without this top-down control, $C_1$'s utilization of $R$ made it a superior competitor, leading to competitive exclusion of $C_2$. Thus, $C_2$'s coexistence in the full community is dependent upon $P$'s presence, implying that

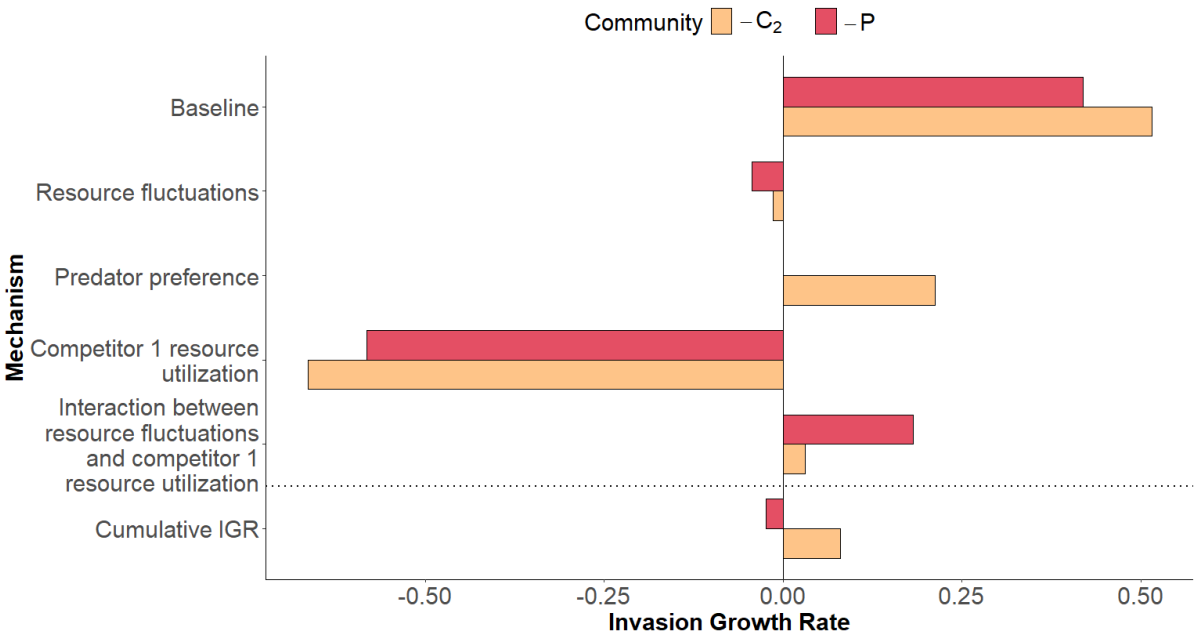


Figure 6: Decomposition of $C_2$'s IGR at the $-C_2$ and $-P$ communities. The sum of all bars of a respective color above the dotted line add to the value of the bar below the dotted line of the respective color. Mechanisms not present in the $-i$ community have no contribution to the IGR and thus have no bar represented.

extinction of $P$ would drive a subsequent loss of $C_2$.

# Discussion

While IGRs have traditionally been used to identify mechanisms of species coexistence, they are increasingly applied to a broader range of ecological phenomena, including priority effects (Ke and Letten, 2018; Grainger et al., 2019a), competitive exclusion (Germain et al., 2018; Shoemaker et al., 2020), and community assembly (Spaak and Schreiber, 2023; Song and Spaak, 2024). We contribute to this expanding body of work by extending key concepts from Modern Coexistence Theory such as IGRs and $-i$ communities to the study of community disassembly. In doing so, we use IGRs to identify secondary extinctions, further demonstrating their utility beyond coexistence analysis (Grainger et al., 2019b).

Our approach to community disassembly relies on an underappreciated cornerstone of Modern Coexistence Theory: $-i$ communities. These communities, introduced by Chesson (1994), correspond to the coexisting species remaining in the long-term after species $i$ is lost. The community disassembly graph introduced here uses this concept recursively, thus describ-

ing the cascading effects of species removals. Because community disassembly graphs are characterized by invasion growth rates, they are the natural counterpart of invasion graphs that describe the possible consequences of invasions by one or multiple species on community structure (Hofbauer and Schreiber, 2022; Spaak and Schreiber, 2023; Godoy et al., 2024; Schreiber, 2025). Moreover, invasion graphs confirm, in a mathematically rigorous manner, an intuitive assumption underlying Modern Coexistence Theory: coexistence (in the sense of permanence) requires that each species has a positive invasion growth rate (IGR) in its $-i$ communities (Grainger et al., 2019a). As illustrated in our applications, secondary extinctions can lead to $-i$ communities where multiple species, not only species $i$, are missing. However, almost all theoretical developments and applications of MCT focus on species whose loss does not lead to secondary extinctions (MacArthur and Levins, 1967; Chesson, 1994; Ellner et al., 2019; Shoemaker et al., 2020; Spaak and Schreiber, 2023).This limitation suggests that MCT frameworks must be expanded to account for systems where species losses trigger cascading extinctions.

Most studies of community disassembly focus on the general robustness of ecological communities to extinction events (Dunne et al., 2002a; Keyes et al., 2024), adopting a broad-scale perspective on the drivers of disassembly. In contrast, we take a fine-scale approach by examining individual cases of secondary extinction and identifying the underlying ecological mechanisms. By applying decomposition techniques from Modern Coexistence Theoryto the appropriately choosen $-i$ communities, we quantify the relative importance of the ecological drivers of secondary extinctions and thereby, extend the utility of these techniques (Chesson, 1994; Ellner et al., 2019).

The applications of these methods demonstrate that secondary extinctions can arise from multiple mechanisms. In the annual plant model (Figure 2), the persistence of *P. erecta* in the presence of *A. wrangelianus* and *H. murinum* relies upon the indirect positive effect of competitors mutually constraining each other's impact on *P. erecta*, and the subadditive impacts of competition on *P. erecta*. Without either factor, *P. erecta* would be unable to coexist with *A. wrangelianus* and *H. murinum*. Similarly, in the grassland system (Figure 4), the secondary extinction of *T. pratense* was driven by both increased direct competition and the loss of direct

facilitation in the disassembled community. These findings support previous studies suggesting that ecological mechanisms and stressors can interact in additive and synergistic ways to influence the likelihood of secondary extinctions (Graham et al., 2011; Colwell et al., 2012; Brodie et al., 2014).

# Challenges and future directions

Our study uses IGRs at multiple $-i$ communities to understand mechanisms driving secondary extinctions. This approach allows us to understand both how the secondarily extinct species coexists in the full community and why it is excluded in the disassembled community. However, the utility of this procedure extends beyond processes of disassembly. For example, in community assembly, the successful invasion of a species from the regional pool might displace resident species (Horn, 1974; Wainright et al., 2021; Zhou et al., 2023). Since the invading species could invade when rare, we know it must have a positive IGR at the pre-invasion community. Furthermore, since the resident species was displaced following introduction of the invading species, we know it must have a negative IGR at the post-invasion community (Schreiber, 2025). Thus, a similar procedure can be followed: decompose the species' IGR in its own $-i$ community to understand how it can invade it to reach the pre-invasion community and decompose its growth rate in the post-invasion community to determine what new attributes of the system drive exclusion following introduction of the new species.

MCT relies on positive growth rates when rare to ensure coexistence i.e. -i communities are invadible. This, however, is only true when the community has no intransitivities (Hofbauer and Schreiber, 2022). A classic example of a coexisting community with intransitivities is a rock-paper-scissors community (May and Leonard, 1975). In this model, no two species can coexist since one always outcompetes the other; however, all three species can coexist together. Due to the competitive intransitivity, species $i$ is incapable of invading its own $-i$ community. Similar dynamics can manifest in higher-dimensional communities (Hofbauer, 1994; Schreiber, 1998; Schreiber and Rittenhouse, 2004; Allesina and Levine, 2011), leaving species susceptible to secondary extinction (Schreiber, 1998; Vandermeer, 2024). Mathematical methods for

handling many of these intransitivities have existed for decades (Hofbauer, 1981; Schreiber, 2000). Although rooted in invasion growth rates, these methods have only recently been incorporated into an MCT partitioning framework for the classical three-species models (Ranjan et al., 2024). These advances hint at the possibility of modifying our framework to account for secondary extinctions in intransitive systems.

Another limitation is that MCT techniques are often uninformative when species exhibit Allee effects, where growth is negative at low densities (Barabás et al., 2018). In our case, while the identification of secondary extinctions is not affected by Allee effects, explaining why a species with an Allee effect goes secondarily extinct requires different methods. This is because such species have negative IGRs in their $-i$ community and consequently cannot return to the pre-extinction community through low-density introductions (Spaak and Schreiber, 2023), rendering the decomposition of low-density growth rates uninformative for assessing full coexistence of the system. However, in some cases, alternatives to IGRs exist for identifying when and why coexistence occurs (Schreiber et al., 2019; Ellner et al., 2022), which raises the possibility that they could be adapted to understand the causes of secondary extinctions.

By applying MCT to community disassembly, we introduce a novel framework to identify secondary extinctions and quantify the underlying driving ecological factors. Moreover, we demonstrate that decomposing IGRs at multiple communities is necessary to understand the directionality and relative importance of the underlying ecological factors. Our work highlights the ever widening utility of invasion growth rates to understand key questions in community ecology.

# Acknowledgments

We would like to thank Marissa Baskett and and John Stachowicz for comments on an early draft. We would also like to thank Raissa D'Souza, Alan Hastings, and Marcel Holyoak for feedback throughout the development of this project. JB was supported by the National Science Foundation Graduate Research Fellowship program under Grant No. DGE-2439024.

# A Parameters and global dynamics of the annual plant model

## A.1 Model and Parameters

The annual plant model from Van Dyke et al. (2022) is

$$x_{i,t+1} = (1 - g_i)s_i x_{i,t} + \frac{g_i \lambda_i x_{i,t}}{1 + \sum_{j=1}^{3} a_{ij} g_j x_{j,t}} \text{ with } 1 \leq i, j \leq 3 \tag{1}$$

where $x_i$ represents the seed density of species $i$.

Let $A$ be the matrix of competition coefficients $a_{ij}$, $\vec{g} = (g_1, g_2, g_3)$ be the vector of germination rates, $\vec{s}$ be the vector of seed survival probabilities, and $\vec{\lambda}$ be the vector of maximum birth rates. The parameters from Van Dyke et al. (2022) are

$$A = \begin{bmatrix} 0.27290462 & 0.9415389 & 0.5590646 \\ 0.13755487 & 0.9483990 & 0.1599514 \\ 0.08483079 & 1.0221670 & 0.4161495 \end{bmatrix}$$

$$\vec{g} = \begin{bmatrix} 0.2240310 & 0.6666667 & 0.6029647 \end{bmatrix}$$

$$\vec{\lambda} = \begin{bmatrix} 2351.5366 & 745.9973 & 654.6758 \end{bmatrix}$$

$$\vec{s} = \begin{bmatrix} 0.2625463 & 0.0450000 & 0.6215016 \end{bmatrix}$$

where species $1, 2,$ and $3$ are *A. wrangelianus*, *H. murinum*, and *P. erecta*, respectively.

## A.2 Solving for attractors of the annual plant model

To identify all the community attractors of the annual plant model (1), we analyze the two subsystems of species using the theory of monotone dynamical systems (Smith, 1995), specifically results for competitive planar maps (Smith, 1998). Then we use invasion graphs (Hofbauer and Schreiber, 2022; Schreiber, 2025) to verify the existence of an attractor that supports all three species.

Ultimately, this analysis only requires solving for the equilibria of (1) and calculating the

IGRs at these equilibria. An equilibrium that supports a subset of species $S \subset \{1, 2, 3\}$ must satisfy

$$1 = (1 - g_i)s_i + \frac{g_i \lambda_i}{1 + \sum_j a_{ij} g_j x_j^*}$$

for all species $i \in S$. Equivalently, it must satisfy the following set of linear equations that are easily solved numerically:

$$\frac{g_i \lambda_i}{1 - (1 - g_i)s_i} - 1 = \sum_j a_{ij} g_j x_j^* \text{ for all } i \in S.$$

### A.2.1 Global dynamics of species pairs

We begin by characterizing the dynamics of any pair of species. Without loss of generality, say $i = 1, 2$. Define the update mapping $P(x) = (P_1(x), P_2(x))$ by

$$P_1(x) = \frac{\lambda_1 g_1 x_1}{1 + g_1 a_{11} x_1 + g_2 a_{12} x_2} + (1 - g_1) s_1 x_1 \text{ and } P_2(x) = \frac{\lambda_2 g_2 x_2}{1 + g_1 a_{21} x_1 + g_2 a_{22} x_2} + (1 - g_2) s_2 x_2.$$

We use results from (Smith, 1998) to characterize the global dynamics. This requires using the theory of monotone maps. The relevant terminology is described in Smith (1995, 1998). First, we verify that (1) with two species ($i = 1, 2$) is strictly competitive in the positive quadrant $(0, \infty)^2$. By Proposition 2.1 in (Smith, 1998) it is sufficient to show that $P_1$ (respectively, $P_2$) is a strictly increasing function of $x_1$ and a strictly decreasing function of $x_2$ (respectively, strictly increasing in $x_2$ and strictly decreasing in $x_1$. To this end, we compute the partial derivatives of $F_1$ and $F_2$ with respect to $x_1$ and $x_2$:

$$\begin{aligned}
\frac{\partial P_1}{\partial x_1} &= \frac{\lambda_1 g_1 (1 + g_2 a_{12} x_2)}{\Delta_1^2} + s_1 \quad \frac{\partial P_1}{\partial x_2} = -\frac{g_2 a_{12} \lambda_1 g_1 x_1}{\Delta_1^2} \\
\frac{\partial P_2}{\partial x_1} &= -\frac{g_1 a_{21} \lambda_2 g_2 x_2}{\Delta_2^2} \quad \frac{\partial P_2}{\partial x_2} = \frac{\lambda_2 g_2 (1 + g_1 a_{21} x_1)}{\Delta_2^2} + s_2 \\
\text{where } \Delta_1 &= 1 + g_1 a_{11} x_1 + g_2 a_{12} x_2 \text{ and } \Delta_2 = 1 + g_1 a_{21} x_1 + g_2 a_{22} x_2.
\end{aligned}$$

As the partial derivatives $\frac{\partial P_i}{\partial x_i}$ are strictly positive in $[0, \infty)^2$ for $i = 1, 2$, the functions $F_i$ increase strictly in $x_i$ in $[0, \infty)^2$. As the partial derivatives $\frac{\partial P_i}{\partial x_j}$ for $i \neq j$ are negative in $(0, \infty)^2$, the functions $F_i$ strictly decrease in $x_j$ ($j \neq i$) in the positive quadrant $(0, \infty)^2$. Hence, by

Proposition 2.3 in (Smith, 1998) , (1) is strictly competitive in the positive quadrant.

Next, we verify hypothesis (H+) in (Smith, 1998) for $P$ on $A = (0, \infty)^2$. This hypothesis consists of four conditions (a)–(d). Condition (a) holds immediately for the competitive ordering $<_K$ on $A$. Condition (b) requires that the determinant of the Jacobian matrix

$$DP(x) = \begin{pmatrix} \frac{\partial P_1}{\partial x_1} & \frac{\partial P_1}{\partial x_2} \\ \frac{\partial P_2}{\partial x_1} & \frac{\partial P_2}{\partial x_2} \end{pmatrix}$$

is positive in $(0, \infty)^2$. The following calculation ensures that this condition is satisfied:

$$\begin{aligned} \Delta_1^2 \Delta_2^2 \det(DP(x)) &= \lambda_1 g_1 \lambda_2 g_2 (1 + g_2 a_{12} x_2)(1 + g_1 a_{21} x_1) + (1 - g_1) s_1 (1 + g_1 a_{21} x_1) \Delta_2 \\ &\quad + (1 - g_2) s_2 (1 + g_2 a_{12} x_2) \Delta_1 + (1 - g_1) s_1 (1 - g_2) s_2 \Delta_1 \Delta_2 \\ &\quad - \lambda_1 g_1 \lambda_2 g_2 g_2 a_{12} g_1 a_{21} x_1 x_2 \\ &= \lambda_1 g_1 \lambda_2 g_2 (1 + g_2 a_{12} x_2 + g_1 a_{21} x_1) + (1 - g_1) s_1 (1 + g_1 a_{21} x_1) \Delta_2 \\ &\quad + (1 - g_2) s_2 (1 + g_2 a_{12} x_2) \Delta_1 + (1 - g_1) s_1 (1 - g_2) s_2 \Delta_1 \Delta_2 \end{aligned}$$

The third condition (c) requires that the diagonal entries of $DP(x)$ be strictly positive and the off-diagonal elements be strictly negative on $(0, \infty)^2$. This follows immediately from our partial derivative calculations. The final condition (d) requires that $P$ is injective in $(0, \infty)^2$. As $\det(DP(x)) > 0$ on $[0, \infty)^2$ and $[0, \infty)^2$ is connected, all points in $(0, \infty)^2$ have the same number of preimages. As the only preimage of $(0, 0)$ is $(0, 0)$, it follows that $P$ is injective.

Having verified these conditions, Corollary 4.4 in (Smith, 1998) implies that all trajectories of (A) for $i = 1, 2$ converge to an equilibrium. To understand which initial conditions converge to which equilibria, we need to solve the equilibria and check the invasion criteria at these equilibria. As we describe below, there is for our parameters at most one equilibrium for any subset of species. Moreover, for any pair of species in the parameterized model, only one of the two mutual invasibility conditions holds. Either both species have a positive invasion growth rate at the other species equilibrium or the invasion growth rates are of opposite sign. When the former occurs, the single species equilibria are unstable (saddles), and there is a unique equilibrium, call it $x^*$, supporting the other two species, i.e. $x_1^* > 0$ and $x_2^* > 0$. Therefore, any

trajectory where initially both species have positive densities converges to $x^*$ i.e. $x^*$ is globally stable. Alternatively, suppose that the invasion growth rates have opposite signs. Without loss of generality, say the invasion growth rate of species $2$ is negative at the equilibrium $(x_1^*, 0)$ of species $1$. Then there is no equilibrium supporting both species and the extinction equilibrium $(0, 0)$ and the species $2$ equilibrium $(0, x_2^*)$ are unstable, while the species $1$ equilibrium is stable. Therefore, Corollary 4.4 implies that all trajectories at which species $1$ is initial present converge to $(x_1^*, 0)$. These results fully characterize the dynamics of all the two species pairs in the three species parameterized model.

### A.2.2 Three species coexistence

We use the invasion graph approach (Figure 7) to verify coexistence in the sense of permanence. This approach was introduced for differential equations in Hofbauer and Schreiber (2022) and extended to flow-kick models that include difference equations in Schreiber (2025). Calculating the equilibria as detailed below for all single and two species subsystems, as described below, and using the convergence results for the single and two species subsystems, one can verify that the invasion graph, as shown in Figure 7, is acyclic and that the invasion growth rate of species $i$ for $i = 1, 2, 3$ is positive at the $-i$ equilibria. Hence, Theorem 4.8 in Schreiber (2025) implies that all three species coexist in the sense of permanence. Numerical simulations suggest that permanence occurs via a global stable equilibrium.

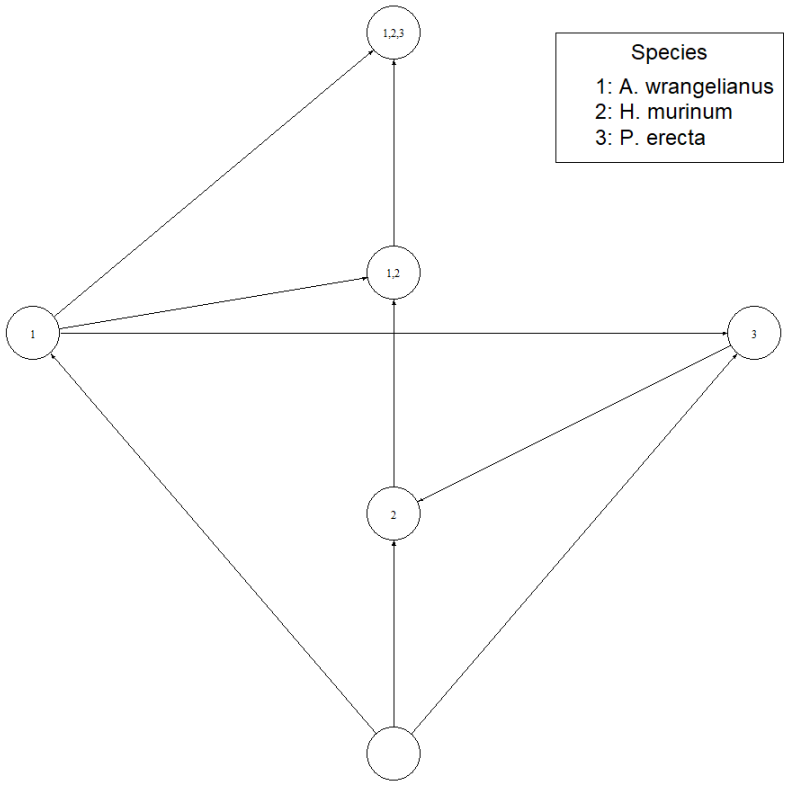


Figure 7: Invasion graph of the annual plant model from Van Dyke et al. (2022). Nodes represent feasible equilibria while directed edges represent changes in community composition as a result of species invasion.

# B Parameters and global dynamics for grassland community model

## B.1 Model and Parameters

The model for the grassland community in Geijzendorffer et al. (2011) discussed in the "Facilitation" section of the main text is

$$\frac{dx_i}{dt} = x_i \left( r_i + \sum_j a_{ij} x_j \right) \tag{2}$$

where $x_i$ is the biomass of species $i$, $r_i$ is the intrinsic growth rate of species $i$, and $a_{ij}$ is the per-capita competitive effect of species $j$ on $i$.

Let $A$ be the matrix of competition coefficients $a_{ij}$ and $\vec{r}$ be the vector of intrinsic growth

rates $r_i$. From Geijzendorffer et al. (2011), the model parameters for *A. stolonifera*, *L. perenne*, *P. pratense*, *T. pratense*, and *T. repens* are respectively

$$\vec{r} = \begin{bmatrix} 0.10077 & 0.04519 & 0.10343 & 0.11271 & 0.07652 \end{bmatrix}^T$$

$$A = \begin{bmatrix} -1.28 & 0.15 & 0.10 & -0.16 & 0.12 \\ 0.13 & -0.41 & -0.12 & 0.03 & 0 \\ -0.38 & -0.30 & -0.41 & -0.15 & -0.11 \\ -0.39 & -0.15 & -0.82 & -0.8 & 0.78 \\ -0.02 & -0.18 & -0.05 & -0.57 & -0.56 \end{bmatrix}$$

## B.2 Solving for attractors of the grassland community model

To determine the global dynamics of the system, we computed the invasion graph Hofbauer and Schreiber (2022) which is shown in Figure 8. This invasion graph is acyclic and all nodes satisfy the permanence condition. Hence, all nodes correspond to global attractors.

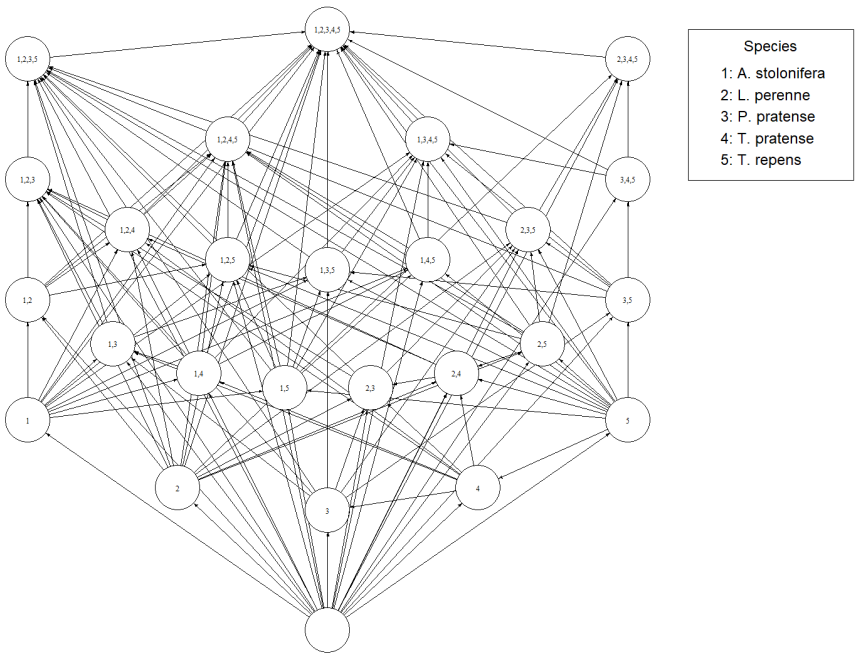


Figure 8: Invasion graph of the grassland community from Geijzendorffer et al. (2011). Nodes represent feasible equilibria while directed edges represent changes in community composition as a result of species invasion.

# C Parameters and global dynamics for diamond model

## C.1 Parameters

Here, we use the same parametrization as Vasseur and Fox (2007) and Shoemaker et al. (2020) for the model of keystone predation described in the "Predation" section of the main text.

| Parameter | Description | Value |
|---|---|---|
| $r$ | Resource intrinsic rate of growth | 1.0 |
| $K$ | Resource carrying capacity | 1.0 |
| $J_{C_1}$ | Competitor 1's ingestion rate | 0.8036 |
| $J_{C_2}$ | Competitor 2's ingestion rate | 0.7 |
| $J_P$ | Predator ingestion rate | 0.4 |
| $M_{C_1}$ | Competitor 1's intrinsic mortality rate | 0.4 |
| $M_{C_2}$ | Competitor 2's intrinsic mortality rate | 0.2 |
| $M_P$ | Predator's intrinsic mortality rate | 0.08 |
| $R_{0_1}$ | Competitor 1's half saturation constant of the resource | 0.16129 |
| $R_{0_2}$ | Competitor 2's half saturation constant of the resource | 0.9 |
| $C_0$ | Predator's half saturation constant of the competitors | 0.5 |
| $\Omega_{PC_1}$ | Predator's prey preference for competitor 1 | 0.92 |
| $\Omega_{C_1R}$ | Competitor 1's preference coefficient for the resource | 1.0 |
| $\Omega_{C_2R}$ | Competitor 2's preference coefficient for the resource | 0.98 |

## C.2 Global dynamics of the diamond model

To assess the global dynamics of the system, we computed numerically estimated all the invasion growth rates and calculated the invasion graph shown in Figure 9. This invasion graph is acyclic and the permanence condition holds for each node. Consequently, each node (community) is supported by a global attractor.

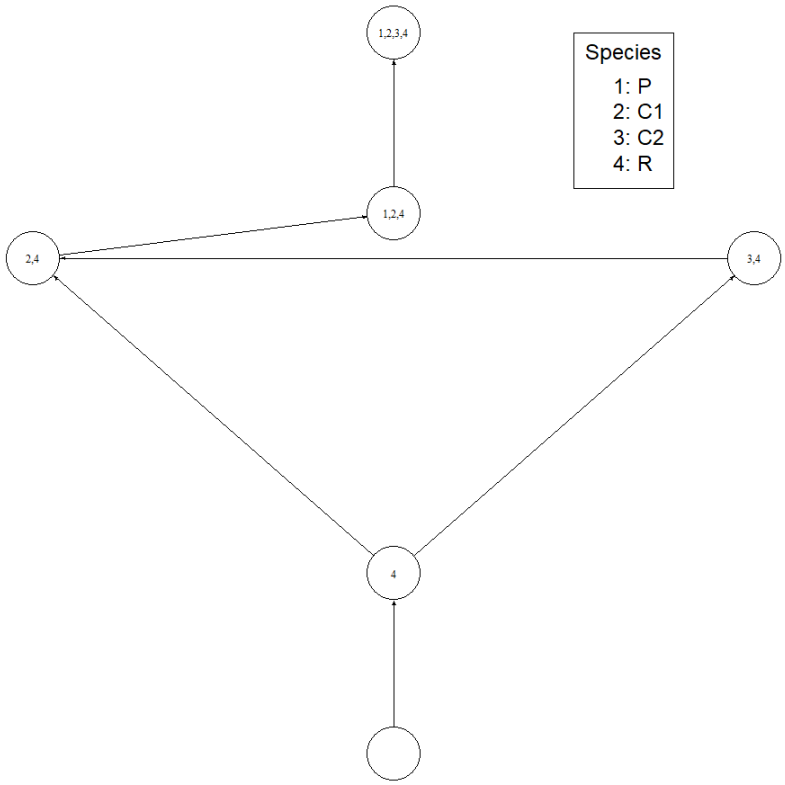


Figure 9: Invasion graph of the diamond model from Vasseur and Fox (2007) and Shoemaker et al. (2020). Nodes represent attractors while directed edges represent changes in community composition as a result of species invasion.

# D Alternative secondary extinction in annual plant model

Revisiting the annual plant model, there exists another secondary extinction event in the full community. As shown in Figure 1A, extinction of *H. murinum* leads to the secondary extinction of *A. wrangelianus*. As the procedure follows, we will (1) understand why *A. wrangelianus* is excluded by *P. erecta* and (2) why it can invade the community with *P. erecta* and *H. murinum* is present.

Figure 1A shows that the -*A. wrangelianus* community has a secondary extinction event of *P. erecta*. Thus, introduction of *A. wrangelianus* alone cannot restore the pre-disassembled community. Thus, we identify a path from the -*A. wrangelianus community* back to the full community. For this empirical example, there exists only one path from -*A. wrangelianus* community to the full community: invasion of *A. wrangelianus* in -*A. wrangelianus* community that changes the composition to coexistence of *A. wrangelianus* and *H. murinum*, followed by

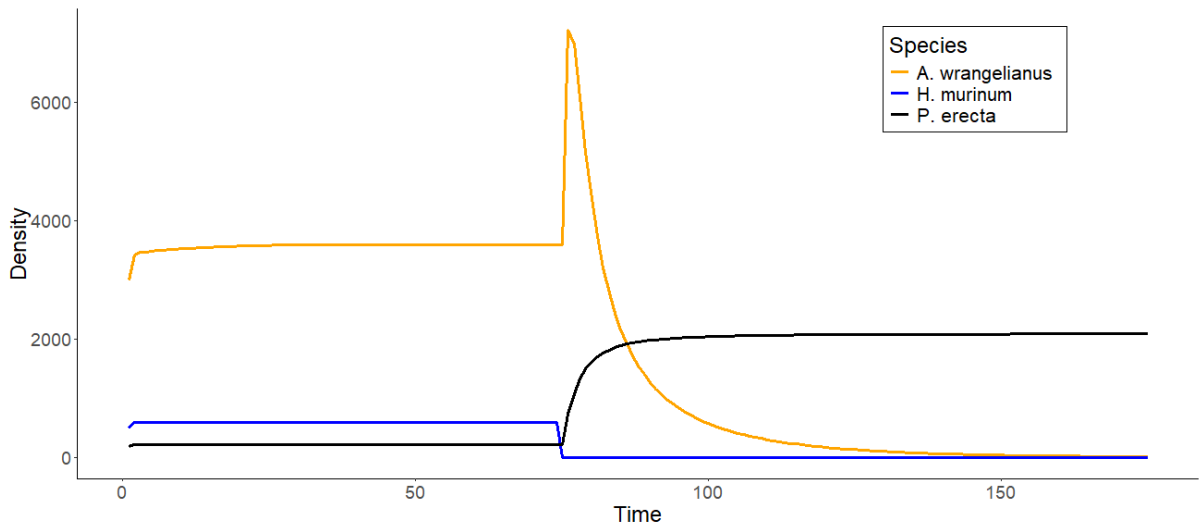


Figure 10: Simulation of community dynamics following extinction of *H. murinum* at time step 75. Note that this leads to a secondary extinction of *A. wrangelianus*, matching the -*H. murinum* predicted in the Community Disassembly Graph in Figure 1A.

invasion of *P. erecta* to reassemble the system back to the full community.

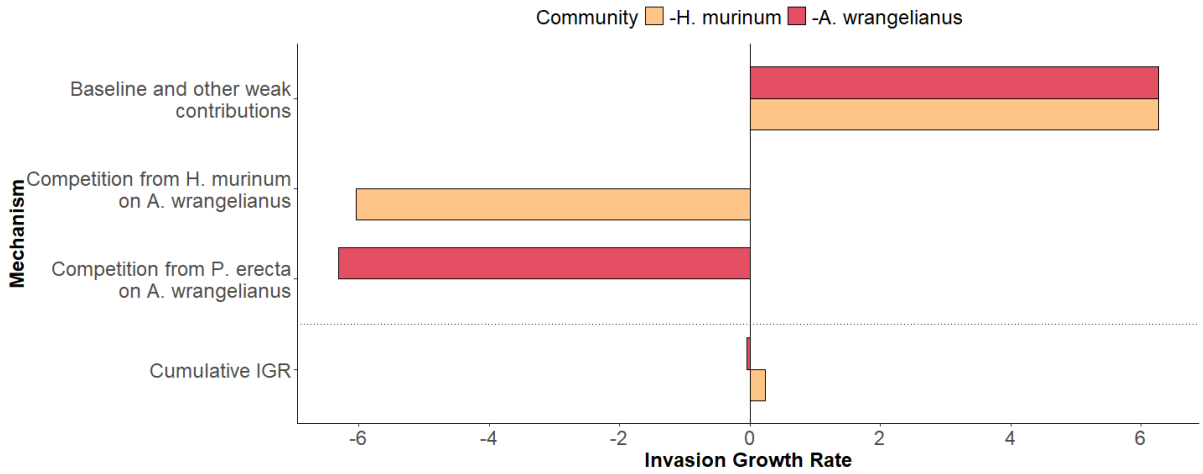


Figure 11: Invasion Growth

Along this assembly path, *A. wrangelianus* only needs to successfully invade once at the -*A. wrangelianus community* since it is not displaced by subsequent invasions on the assembly path. Thus, we simply decompose the invasion growth rate of *A. wrangelianus* at the -*A. wrangelianus* community to understand why it successfully invades in this community.

As shown in Figure 12, *A. wrangelianus* can invade the $-$*A. wrangelianus* community, only containing *H. murinum*. Furthermore, since *H. murinum* has a positive invasion growth rate in the community only containing *A. wrangelianus*, we know they coexist through mutual

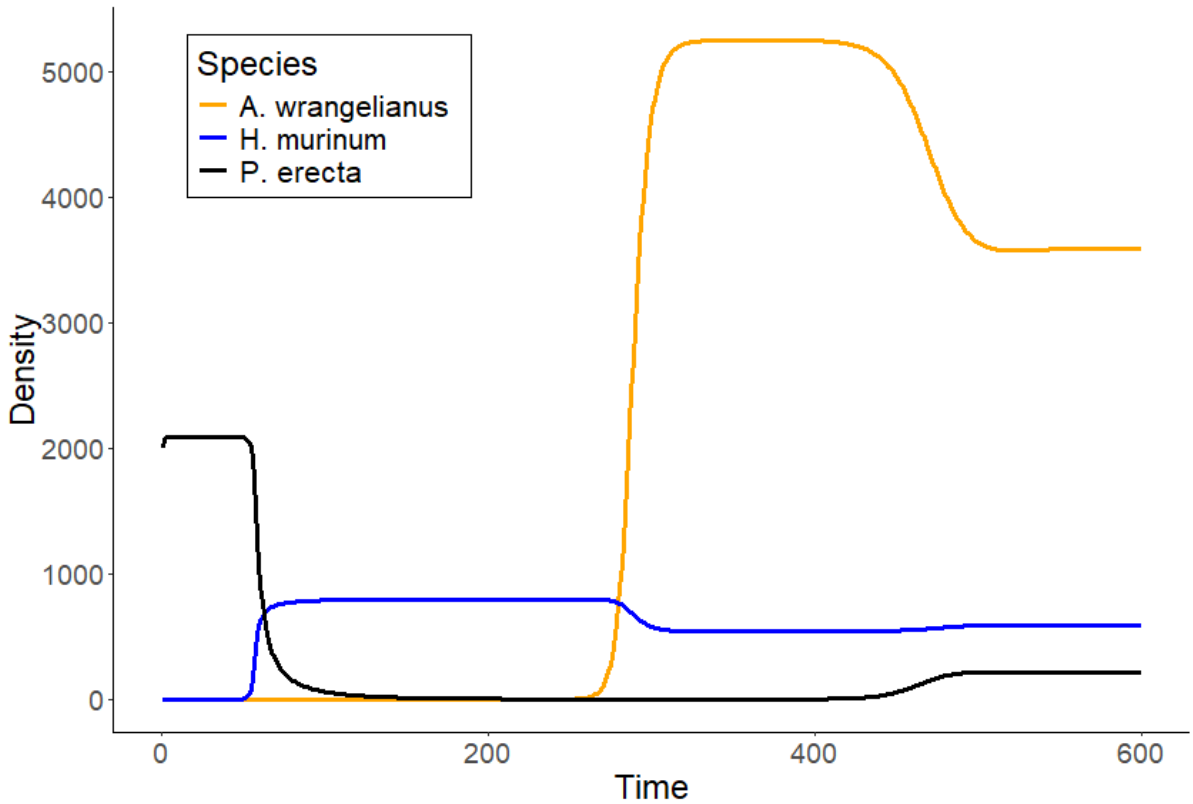


Figure 12: Simulation of dynamics associated with invasion. Invasion of *H. murinum* at time step 50; invasion of *A. wrangelianus* at time step 250; invasion of *P. erecta* at time step 400.

invasibility.

In the disassembled community, *A. wrangelianus* cannot coexist with *P. erecta* since *P. erecta* is a superior competitor to *A. wrangelianus*. However, despite this, we find that *A. wrangelianus* and *H. murinum* can coexist. When *P. erecta* then invades the community with *A. wrangelianus* and *H. murinum*, it invades without displacing *A. wrangelanius* due to *H. murinum*'s competitive pressure on *P. erecta*, leading to coexistence of the full community. Thus, we see that persistence of *A. wrangelianus* in the full community is contingent upon the presence of *H. murinum*.

# References


S. Allesina and J. M. Levine. A competitive network theory of species diversity. Proceedings of the National Academy of Sciences, 108(14):5638–5642, 2011.

R. A. Armstrong and R. McGehee. Competitive exclusion. The American Naturalist, 115(2): 151–170, 1980.

C. E. Aslan, E. S. Zavaleta, B. Tershy, and D. Croll. Mutualism disruption threatens global plant biodiversity: a systematic review. PloS one, 8(6):e66993, 2013.

M. S. Bane, M. J. Pocock, and R. James. Effects of model choice, network structure, and interaction strengths on knockout extinction models of ecological robustness. Ecology and evolution, 8(22):10794–10804, 2018.

G. Barabás, R. D'Andrea, and S. M. Stump. Chesson's coexistence theory. Ecological monographs, 88(3):277–303, 2018.

J. Bascompte and D. B. Stouffer. The assembly and disassembly of ecological networks. Philosophical Transactions of the Royal Society B: Biological Sciences, 364(1524):1781–1787, 2009.

J. F. Brodie, C. E. Aslan, H. S. Rogers, K. H. Redford, J. L. Maron, J. L. Bronstein, and C. R. Groves. Secondary extinctions of biodiversity. Trends in ecology & evolution, 29(12):664–672, 2014.

P. Chesson. Multispecies competition in variable environments. Theoretical population biology, 45(3):227–276, 1994.

A. T. Clark, L. G. Shoemaker, J.-F. Arnoldi, G. Barabás, R. Germain, O. Godoy, L. Hallett, C. Karakoç, S. Saavedra, and S. Schreiber. A practical guide to quantifying ecological coexistence. 2024.

R. K. Colwell, R. R. Dunn, and N. C. Harris. Coextinction and persistence of dependent species in a changing world. Annual Review of Ecology, Evolution, and Systematics, 43(1): 183–203, 2012.

J. A. Dunne, R. J. Williams, and N. D. Martinez. Food-web structure and network theory: the role of connectance and size. Proceedings of the National Academy of Sciences, 99(20): 12917–12922, 2002a.

J. A. Dunne, R. J. Williams, and N. D. Martinez. Network structure and biodiversity loss in food webs: robustness increases with connectance. Ecology letters, 5(4):558–567, 2002b.

J. A. Dunne, R. J. Williams, and N. D. Martinez. Network structure and robustness of marine food webs. Marine Ecology Progress Series, 273:291–302, 2004.

B. Ebenman and T. Jonsson. Using community viability analysis to identify fragile systems and keystone species. Trends in Ecology & Evolution, 20(10):568–575, 2005.

K. F. Edwards and S. J. Schreiber. Preemption of space can lead to intransitive coexistence of competitors. Oikos, 119(7):1201–1209, 2010.

S. P. Ellner, R. E. Snyder, P. B. Adler, and G. Hooker. An expanded modern coexistence theory for empirical applications. Ecology letters, 22(1):3–18, 2019.

S. P. Ellner, R. E. Snyder, P. B. Adler, and G. Hooker. Toward a "modern coexistence theory"' for the discrete and spatial. Ecological Monographs, 92(4):e1548, 2022.

G. F. Gause. The struggle for existence. 1934.

I. Geijzendorffer, W. Van der Werf, F. Bianchi, and R. Schulte. Sustained dynamic transience in a lotka–volterra competition model system for grassland species. Ecological Modelling, 222(15):2817–2824, 2011.

R. M. Germain, J. L. Williams, D. Schluter, and A. L. Angert. Moving character displacement beyond characters using contemporary coexistence theory. Trends in Ecology & Evolution, 33(2):74–84, 2018.

P. W. Glynn. Some physical and biological determinants of coral community structure in the eastern pacific. Ecological monographs, 46(4):431–456, 1976.

O. Godoy, F. Soler-Toscano, J. R. Portillo, and J. A. Langa. The assembly and dynamics of ecological communities in an ever-changing world. Ecological Monographs, 94(4):e1633, 2024.

N. A. Graham, P. Chabanet, R. D. Evans, S. Jennings, Y. Letourneur, M. Aaron MacNeil, T. R. McClanahan, M. C. Öhman, N. V. Polunin, and S. K. Wilson. Extinction vulnerability of coral reef fishes. Ecology letters, 14(4):341–348, 2011.

T. N. Grainger, A. D. Letten, B. Gilbert, and T. Fukami. Applying modern coexistence theory to priority effects. proceedings of the national academy of sciences, 116(13):6205–6210, 2019a.

T. N. Grainger, J. M. Levine, and B. Gilbert. The invasion criterion: a common currency for ecological research. Trends in ecology & evolution, 34(10):925–935, 2019b.

J. Hofbauer. A general cooperation theorem for hypercycles. Monatshefte für Mathematik, 91 (3):233–240, 1981.

J. Hofbauer. Heteroclinic cycles in ecological differential equations. Equadiff 8, pages 105–116, 1994.

J. Hofbauer and S. J. Schreiber. Permanence via invasion graphs: incorporating community assembly into modern coexistence theory. Journal of mathematical biology, 85(5):54, 2022.

J. Hofbauer and K. Sigmund. Evolutionary games and population dynamics. Cambridge university press, 1998.

H. S. Horn. The ecology of secondary succession. Annual review of ecology and systematics, pages 25–37, 1974.

J. Jackson and L. Buss. Alleopathy and spatial competition among coral reef invertebrates. Proceedings of the National Academy of Sciences, 72(12):5160–5163, 1975.

F. Jordán. Keystone species and food webs. Philosophical Transactions of the Royal Society B: Biological Sciences, 364(1524):1733–1741, 2009.

P.-J. Ke and A. D. Letten. Coexistence theory and the frequency-dependence of priority effects. Nature Ecology & Evolution, 2(11):1691–1695, 2018.

R. Kehoe, E. Frago, and D. Sanders. Cascading extinctions as a hidden driver of insect decline. Ecological Entomology, 46(4):743–756, 2021.

B. Kerr, M. A. Riley, M. W. Feldman, and B. J. Bohannan. Local dispersal promotes biodiversity in a real-life game of rock–paper–scissors. Nature, 418(6894):171–174, 2002.

A. A. Keyes, A. K. Barner, and L. E. Dee. Synthesising the relationships between food web structure and robustness. Ecology Letters, 27(10):e14533, 2024.

R. E. Langendorf, J. A. Estes, J. C. Watson, M. C. Kenner, B. B. Hatfield, M. T. Tinker, E. Waddle, M. L. DeMarche, and D. F. Doak. Dynamic and context-dependent keystone species effects in kelp forests. Proceedings of the National Academy of Sciences, 122(10): e2413360122, 2025.

M. Letnic, F. Koch, C. Gordon, M. S. Crowther, and C. R. Dickman. Keystone effects of an alien top-predator stem extinctions of native mammals. Proceedings of the Royal Society B: Biological Sciences, 276(1671):3249–3256, 2009.

J. M. Levine, J. Bascompte, P. B. Adler, and S. Allesina. Beyond pairwise mechanisms of species coexistence in complex communities. Nature, 546(7656):56–64, 2017.

J. Lubchenco. Plant species diversity in a marine intertidal community: importance of herbivore food preference and algal competitive abilities. The American Naturalist, 112(983):23–39, 1978.

R. MacArthur and R. Levins. The limiting similarity, convergence, and divergence of coexisting species. The american naturalist, 101(921):377–385, 1967.

M. Manhart and E. I. Shakhnovich. Growth tradeoffs produce complex microbial communities on a single limiting resource. Nature communications, 9(1):3214, 2018.

R. M. May and W. J. Leonard. Nonlinear aspects of competition between three species. SIAM journal on applied mathematics, 29(2):243–253, 1975.

K. McCann, A. Hastings, and G. R. Huxel. Weak trophic interactions and the balance of nature. Nature, 395(6704):794–798, 1998.

J. Memmott, N. M. Waser, and M. V. Price. Tolerance of pollination networks to species extinctions. Proceedings of the Royal Society of London. Series B: Biological Sciences, 271 (1557):2605–2611, 2004.

M. L. Moir, P. A. Vesk, K. E. Brennan, D. A. Keith, L. Hughes, and M. A. McCARTHY. Current constraints and future directions in estimating coextinction. Conservation Biology, 24(3):682–690, 2010.

S. D. Mylius and O. Diekmann. The resident strikes back: invader-induced switching of resident attractor. Journal of Theoretical Biology, 211(4):297–311, 2001.

S. D. Mylius, M. Doebeli, and O. Diekmann. Can initial invasion dynamics correctly predict phenotypic substitutions. Advances in Adaptive Dynamics, U. Dieckmann & JAJ Metz (eds.), to appear, 1998.

R. S. Ostfeld and K. LoGiudice. Community disassembly, biodiversity loss, and the erosion of an ecosystem service. Ecology, 84(6):1421–1427, 2003.

R. T. Paine. Food web complexity and species diversity. The American Naturalist, 100(910): 65–75, 1966.

R. T. Paine. Food webs: linkage, interaction strength and community infrastructure. Journal of animal ecology, 49(3):667–685, 1980.

R. T. Paine, J. Terborgh, and J. Estes. Food chain dynamics and trophic cascades in intertidal habitats. Trophic cascades: predators, prey, and the changing dynamics of nature, pages 21–35, 2010.

A. I. Pastore, G. Barabás, M. D. Bimler, M. M. Mayfield, and T. E. Miller. The evolution of niche overlap and competitive differences. Nature Ecology & Evolution, 5(3):330–337, 2021.

S. C. Pennings and R. M. Callaway. Impact of a parasitic plant on the structure and dynamics of salt marsh vegetation. Ecology, 77(5):1410–1419, 1996.

R. Ranjan, T. Koffel, and C. A. Klausmeier. The three-species problem: Incorporating competitive asymmetry and intransitivity in modern coexistence theory. Ecology Letters, 27(4): e14426, 2024.

S. J. Schreiber. On the stabilizing effect of specialist predators on founder-controlled communities. Canadian Applied Math. Quart, 6:195–206, 1998.

S. J. Schreiber. Criteria for $C^r$ robust permanence. Journal of Differential Equations, 162(2): 400–426, 2000.

S. J. Schreiber. Persistence despite perturbations for interacting populations. Journal of Theoretical Biology, 242(4):844–852, 2006.

S. J. Schreiber. Coexistence and extinction in flow-kick systems: An invasion growth rate approach. arXiv preprint arXiv:2507.02157, 2025.

S. J. Schreiber and S. Rittenhouse. From simple rules to cycling in community assembly. Oikos, 105(2):349–358, 2004.

S. J. Schreiber, M. Yamamichi, and S. Y. Strauss. When rarity has costs: coexistence under positive frequency-dependence and environmental stochasticity. Ecology, 100(7):e02664, 2019.

L. G. Shoemaker, A. K. Barner, L. S. Bittleston, and A. I. Teufel. Quantifying the relative importance of variation in predation and the environment for species coexistence. Ecology Letters, 23(6):939–950, 2020.

H. L. Smith. Monotone dynamical systems: An introduction to the theory of competitive and cooperative systems. Number 41. American Mathematical Society, 1995.

H. L. Smith. Planar competitive and cooperative difference equations. Journal of Difference Equations and Applications, 3(5-6):335–357, 1998.

K. Soetaert, T. Petzoldt, and R. W. Setzer. Solving differential equations in r: package desolve. Journal of statistical software, 33:1–25, 2010.

C. Song and J. W. Spaak. Trophic tug-of-war: Coexistence mechanisms within and across trophic levels. Ecology Letters, 27(4):e14409, 2024.

J. W. Spaak and S. J. Schreiber. Building modern coexistence theory from the ground up: the role of community assembly. Ecology Letters, 26(11):1840–1861, 2023.

J. J. Stachowicz. Mutualism, facilitation, and the structure of ecological communities: positive interactions play a critical, but underappreciated, role in ecological communities by reducing physical or biotic stresses in existing habitats and by creating new habitats on which many species depend. Bioscience, 51(3):235–246, 2001.

J. J. Stachowicz and M. E. Hay. Mutualism and coral persistence: the role of herbivore resistance to algal chemical defense. Ecology, 80(6):2085–2101, 1999.

G. Strona and C. J. Bradshaw. Co-extinctions annihilate planetary life during extreme environmental change. Scientific reports, 8(1):16724, 2018.

Y. Tang, F. Wang, and W. Zhou. Network structure indicators predict ecological robustness in food webs. Ecological Research, 39(5):766–774, 2024.

D. Tilman. Resource competition and community structure. Number 17. Princeton university press, 1982.

M. N. Van Dyke, J. M. Levine, and N. J. Kraft. Small rainfall changes drive substantial changes in plant coexistence. Nature, 611(7936):507–511, 2022.

A. J. Vanbergen, B. A. Woodcock, M. S. Heard, and D. S. Chapman. Network size, structure and mutualism dependence affect the propensity for plant–pollinator extinction cascades. Functional ecology, 31(6):1285–1293, 2017.

J. Vandermeer. Transitive and intransitive structures in competition-based ecological communities. Ecological Complexity, 60:101103, 2024.

D. A. Vasseur and J. W. Fox. Environmental fluctuations can stabilize food web dynamics by increasing synchrony. Ecology letters, 10(11):1066–1074, 2007.

C. A. Wainright, C. C. Muhlfeld, J. J. Elser, S. L. Bourret, and S. P. Devlin. Species invasion progressively disrupts the trophic structure of native food webs. Proceedings of the National Academy of Sciences, 118(45):e2102179118, 2021.

A. D. Wallach, W. J. Ripple, and S. P. Carroll. Novel trophic cascades: apex predators enable coexistence. Trends in Ecology & Evolution, 30(3):146–153, 2015.

J. P. Wright, C. G. Jones, and A. S. Flecker. An ecosystem engineer, the beaver, increases species richness at the landscape scale. Oecologia, 132:96–101, 2002.

J. D. Yeakel, M. M. Pires, M. A. de Aguiar, J. L. O'Donnell, P. R. Guimarães Jr, D. Gravel, and T. Gross. Diverse interactions and ecosystem engineering can stabilize community assembly. Nature communications, 11(1):3307, 2020.

E. Zavaleta, J. Pasari, J. Moore, D. Hernandez, K. B. Suttle, and C. C. Wilmers. Ecosystem responses to community disassembly. Annals of the New York Academy of Sciences, 1162 (1):311–333, 2009.

L. Zhou, W. Liu, L. Bai, H. Liu, J. Wang, X. Ma, L. Huang, K. Guo, H. Yu, and J. Hu. Female's war: a story of the invasion and competitive displacement between two xylophilus group nematode species. Journal of Pest Science, 96(3):1301–1311, 2023.